J|A|C|S
ARTICLES
Published on Web 05/26/2007

Influence of Environment on the Electronic Structure of Cob(III)alamins: Time-Resolved Absorption Studies of the S_1 State Spectrum and Dynamics

D. Ahmasi Harris,[§] Andrew B. Stickrath,[§] Elizabeth C. Carroll,[†,§] and Roseanne J. Sension*[,†,‡,§]

Contribution from the FOCUS Center, Department of Chemistry, and Program in Applied Physics, University of Michigan, Ann Arbor, Michigan 48109

Received August 25, 2006; E-mail: rsension@umich.edu

Abstract: Transient absorption spectroscopy has been used to elucidate the nature of the S_1 intermediate state populated following excitation of cob(III)alamin (Cbl(III)) compounds. This state is sensitive both to axial ligation and to solvent polarity. The excited-state lifetime as a function of temperature and solvent environment is used to separate the dynamic and electrostatic influence of the solvent. Two distinct types of excited states are identified, both assigned to π3d configurations. The spectra of both types of excited states are characterized by a red absorption band (ca. 600 nm) assigned to Co 3d → 3d or Co 3d → corrin π^* transitions and by visible absorption bands similar to the corrin $\pi \rightarrow \pi^*$ transitions observed for ground state Cbl(III) compounds. The excited state observed following excitation of nonalkyl Cbl(III) compounds has an excited-state spectrum characteristic of Cbl(III) molecules with a weakened bond to the axial ligand (Type I). A similar excited-state spectrum is observed for adenosylcobalamin (AdoCbl) in water and ethylene glycol. The excited-state spectrum of methyl, ethyl, and *n*-propylcobalamin is characteristic of a Cbl(III) species with a σ-donating alkyl anion ligand (Type II). This Type II excited-state spectrum is also observed for AdoCbl bound to glutamate mutase. The results are discussed in the context of theoretical calculations of Cbl(III) species reported in the literature and highlight the need for additional calculations exploring the influence of the alkyl ligand on the electronic structure of cobalamins.

Introduction

Vitamin B_{12} or cyanocobalamin (CNCbl) is an important biological cofactor and an essential human nutrient.[1] Two B_{12} dependent human enzymes, methylmalonyl-CoA mutase and methionine synthase, incorporate active alkylcobalamins derived from CNCbl. Methylcobalamin (MeCbl) functions as a methyl cation donor in methionine synthase, with heterolytic cleavage of the cobalt−carbon bond to form cob(I)alamin.[2,3] Adenosylcobalamin-dependent (coenzyme B_{12}, AdoCbl) enzymes catalyze rearrangement reactions that proceed via mechanisms involving organic radicals generated by homolysis of the coenzyme cobalt−carbon bond to produce an adenosyl radical and cob(II)alamin.[3,4] Finke and co-workers have determined a bond dissociation energy (BDE) for AdoCbl in ethylene glycol of 134 kJ/mol,[5,6] with a half-life for bond dissociation of *ca*. 6 months at physiological temperatures. On the other hand, enzymatic turnover requires bond dissociation lifetimes of *ca.* 10 ms or less.[7,8] Thus the protein accelerates bond homolysis by approximately 12 orders of magnitude.

The influence of the protein environment facilitating the homolysis or heterolysis of the Co−C bond remains a significant open question. Likewise, the role of the alkyl group, Me or Ado, in the reaction is uncertain. Clearly the methyl transfer reaction requires MeCbl, but why do radical rearrangement reactions require AdoCbl? How does the protein enhance homolysis and inhibit heterolysis in AdoCbl-dependent enzymes, while homolysis is inhibited in structurally similar MeCbl enzymes? The bond dissociation energy of MeCbl is ca. 16% higher than that of AdoCbl (155 ± 12 kJ/mol vs 134 kJ/mol).[9−11] This difference in BDE may help suppress bond homolysis in methyl transferase enzymes. However, it does not account for the acceleration of homolysis in AdoCbl-dependent enzymes.

The electronic and vibrational spectra of cobalamins are characteristic of both oxidation state and axial ligation of the cobalt ion central to cobalamins. The influence on the electronic spectrum is illustrated in Figure 1. A number of recent studies have been designed and carried out to use spectroscopic techniques to explore the ways in which a protein environment may affect the reactive Co−C bond. These studies have employed a wide variety of complementary techniques, includ-

[†] FOCUS Center.
[‡] Department of Chemistry.
[§] Program in Applied Physics.

(1) *B12*; Dolphin, D., Ed.; John Wiley and Sons: New York, 1982; Vol. 1.
(2) Banerjee, R.; Matthews, R. G. *FASEB J.* **1990**, *4*, 1450−1459.
(3) Ludwig, M. L.; Matthews, R. G. *Ann. Rev. Biochem.* **1997**, *66*, 269−313.
(4) Marsh, E. N. G. *Essays Biochem.* **1999**, *34*, 139−154.
(5) Hay, B. P.; Finke, R. G. *Polyhedron* **1988**, *7*, 1469−1481.
(6) Hay, B. P.; Finke, R. G. *J. Am. Chem. Soc.* **1986**, *108*, 4820−4829.
(7) Marsh, E. N. G.; Ballou, D. P. *Biochemistry* **1998**, *37*, 11864−11872.
(8) Padmakumar, R.; Padmakumar, R.; Banerjee, R. *Biochemistry* **1997**, *36*, 3713−3718.
(9) Martin, B. D.; Finke, R. G. *J. Am. Chem. Soc.* **1990**, *112*, 2419−2420.
(10) Martin, B. D.; Finke, R. G. *J. Am. Chem. Soc.* **1992**, *114*, 585−592.
(11) Hung, R. R.; Grabowski, J. J. *J. Am. Chem. Soc.* **1999**, *121*, 1359−1364.

10.1021/ja066197y CCC: $37.00

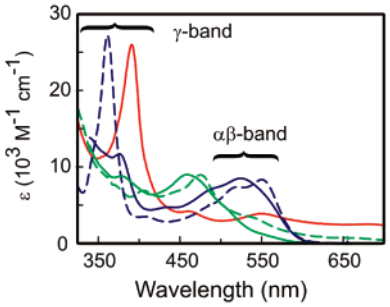

Figure 1. Representative ground state absorption spectra of cobalamins: Cob(I)alamin, solid red line; cob(II)alamin, dashed green line; base-off AdoCbl, solid green line; AdoCbl, solid blue line; and CNCbl, dashed blue line.

ing resonance Raman spectroscopy,[12−15] low temperature absorption and magnetic circular dichroism spectroscopies,[16−20] time-resolved IR spectroscopy,[21] and time-resolved UV−visible absorption spectroscopy.[21−29] The experimental studies suggest that the influence of the protein environment on AdoCbl in general, and the Co−C bond in particular, is subtle. Resonance Raman studies of AdoCbl and other alkylcobalamins found little change in Co−C bond stretching frequency.[14,15,30] Thus the influence of the protein environment is not a straightforward protein-induced bond weakening.

Theoretical studies of cobalamin structure and reactivity have also provided some important insights into the enzyme mechanism. The development of powerful density functional (DFT) methods allows realistic modeling of cobalamins, and a number of groups have investigated the influence of trans axial ligands and corrin ring distortion on the Co−C bond.[16,31−39] A small inverse trans effect of the axial ligand on the Co−C bond is reported, but no strong influence is revealed. These studies suggest that steric mechanisms, including Co−N axial bond elongation and angular distortion of the corrin ring, are not responsible for activation of the Co−C bond toward homolysis, although the influence of the protein on the trans axial ligand may act to inhibit heterolysis of the Co−C bond. It has also been suggested that the initial activation of the Co−C bond is determined by the electrostatic influence of the protein matrix on the coenzyme.[31] In this model the electrostatic field generated by polar amino acids of the protein assists electron reorganization between the cobalt and the axial ligands and leads to labilization of the Co−C bond.

Transient absorption studies have investigated the nature of the intermediate states populated following excitation of both alkyl- and nonalkylcob(III)alamin species.[21−29] The evolution of the spectrum probes the influence of the environment and ligation on the electronic states of cobalamins in regions of conformational space characteristic of the excited-state minima, away from the stable ground state geometry. In many cases, the states probed are "dark" states unobserved in the linear absorption spectrum. Thus these measurements probe the influence of environment on electronic structure in a manner that complements rather than duplicates the information obtained in the resonance Raman, low-temperature absorption, and magnetic circular dichroism experiments reported by others.[12−20] This paper extends our earlier studies of the excited states of cobalamins by exploring the influence of environment and ligation on the spectrum of the S_1 state. The influence of temperature on excited-state lifetime and dynamics is used as a tool to provide additional insight into the nature of this state. The results of these measurements are discussed in the context of prior experiments to elucidate the influence of environment on the electronic structure of cobalamins in general and the influence of the protein environment in Glutamate Mutase (GlmES) on AdoCbl in particular.

Experimental Methods

Adenosylcobalamin, methylcobalamin, and cyanocobalamin were obtained from Sigma-Aldrich and used without further purification. All cobalamin samples were prepared to a concentration of 2 mM in either an aqueous solution or a solution of ethylene glycol. The solutions were prepared, stored, and studied under anaerobic conditions. For aqueous cobalamin solutions, nitrogen gas was bubbled through doubly distilled water for a minimum of 1 h to deoxygenate the solvent before adding the cobalamin. For cobalamin solutions in ethylene glycol, a freeze−pump−thaw cycle was repeated three or four times to deoxygenate the ethylene glycol. During measurements, all cobalamin samples were maintained under a positive pressure atmosphere of nitrogen to exclude oxygen.

Temperature control was achieved by immersing the sample reservoir in a bath with a 50/50 mixture of water and ethylene glycol. The temperature of the bath was controlled by a Neslab RTE-111 Refriger-

(12) Dong, S.; Padmakumar, R.; Banerjee, R.; Spiro, T. G. *J. Am. Chem. Soc.* **1996**, *118*, 9182−9183.
(13) Dong, S.; Padmakumar, R.; Banerjee, R.; Spiro, T. G. *Inorg. Chim. Acta* **1998**, *270*, 392−398.
(14) Dong, S.; Padmakumar, R.; Banerjee, R.; Spiro, T. G. *J. Am. Chem. Soc.* **1999**, *121*, 7063−7070.
(15) Dong, S.; Padmakumar, R.; Maiti, N.; Banerjee, R.; Spiro, T. G. *J. Am. Chem. Soc.* **1998**, *120*, 9947−9948.
(16) Brooks, A. J.; Vlasie, M.; Banerjee, R.; Brunold, T. C. *J. Am. Chem. Soc.* **2004**, *126*, 8167−8180.
(17) Stich, T. A.; Brooks, A. J.; Buan, N. R.; Brunold, T. C. *J. Am. Chem. Soc.* **2003**, *125*, 5897−5914.
(18) Stich, T. A.; Buan, N. R.; Brunold, T. C. *J. Am. Chem. Soc.* **2004**, *126*, 9735−9749.
(19) Brooks, A. J.; Vlasie, M.; Banerjee, R.; Brunold, T. C. *J. Am. Chem. Soc.* **2005**, *127*, 16522−16528.
(20) Brooks, A. J.; Fox, C. C.; Marsh, E. N. G.; Vlasie, M.; Banerjee, R.; Brunold, T. C. *Biochemistry* **2005**, *44*, 15167−15181.
(21) Shiang, J. J.; Cole, A. G.; Sension, R. J.; Hang, K.; Weng, Y.; Trommel, J. S.; Marzilli, L. G.; Lian, T. *J. Am. Chem. Soc.* **2006**, *128*, 801−808.
(22) Walker, L. A., II; Jarrett, J. T.; Anderson, N. A.; Pullen, S. H.; Matthews, R. G.; Sension, R. J. *J. Am. Chem. Soc.* **1998**, *120*, 3597−3603.
(23) Walker, L. A., II; Shiang, J. J.; Anderson, N. A.; Pullen, S. H.; Sension, R. J. *J. Am. Chem. Soc.* **1998**, *120*, 7286−7292.
(24) Shiang, J. J.; Walker, L. A., II; Anderson, N. A.; Cole, A. G.; Sension, R. J. *J. Phys. Chem. B* **1999**, *103*, 10532−10539.
(25) Yoder, L. M.; Cole, A. G.; Walker, L. A., II; Sension, R. J. *J. Phys. Chem. B* **2001**, *105*, 12180−12188.
(26) Cole, A. G.; Yoder, L. M.; Shiang, J. J.; Anderson, N. A.; Walker, L. A., II; Banaszak Holl, M. M.; Sension, R. J. *J. Am. Chem. Soc.* **2002**, *124*, 434−441.
(27) Sension, R. J.; Cole, A. G.; Harris, A. D.; Fox, C. C.; Woodbury, N. W.; Lin, S.; Marsh, E. N. G. *J. Am. Chem. Soc.* **2004**, *126*, 1598−1599.
(28) Sension, R. J.; Harris, D. A.; Stickrath, A.; Cole, A. G.; Fox, C. C.; Marsh, E. N. G. *J. Phys. Chem. B* **2005**, *109*, 18146−18152.
(29) Sension, R. J.; Harris, D. A.; Cole, A. G. *J. Phys. Chem. B* **2005**, *109*, 21954−21962.
(30) Huhta, M. S.; Chen, H.-P.; Hemann, C.; Hille, C. R.; Marsh, E. N. G. *Biochem. J.* **2001**, *355*, 131−137.
(31) Andruniow, T.; Zgierski, M. Z.; Kozlowski, P. M. *J. Phys. Chem. B* **2000**, *104*, 10921−10927.
(32) Andruniow, T.; Zgierski, M. Z.; Kozlowski, P. M. *Chem. Phys. Lett.* **2000**, *331*, 509−512.
(33) Andruniow, T.; Zgierski, M. Z.; Kozlowski, P. M. *J. Am. Chem. Soc.* **2001**, *123*, 2679−2680.
(34) Dolker, N.; Maseras, F.; Lledos, A. *J. Phys. Chem. B* **2001**, *105*, 7564−7571.
(35) Jensen, K. P.; Sauer, S. P. A.; Liljefors, T.; Norrby, P.-O. *Organometallics* **2001**, *20*, 550−556.
(36) Jensen, K. P.; Ryde, U. *THEOCHEM* **2002**, *585*, 239−255.
(37) Dolker, N.; Maseras, F.; Lledos, A. *J. Phys. Chem. B* **2003**, *107*, 306−315.
(38) Ouyang, L.; Randaccio, L.; Rulis, P.; Kurmaev, E. Z.; Moewes, A.; Ching, W. Y. *THEOCHEM* **2003**, *622*, 221−227.
(39) Kozlowski, P. M.; Zgierski, M. Z. *J. Phys. Chem. B* **2004**, *108*, 14163−14170.

ated Bath/Circulator, capable of maintaining temperatures from −25 °C to +150 °C. The samples were flowed through a 1 mm path length cell to refresh the sample volume between laser pulses, and the temperature was measured with a temperature probe inserted in a T-joint located immediately after the sample cell. The temperature of the solvent was varied from 8 °C to 80 °C and was maintained within ±0.5 °C.

Pump−probe transient absorption experiments were performed using 0.3 mJ laser pulses from a 1 kHz titanium-sapphire laser system in the manner described previously.[21,29] All samples were pumped with the second harmonic of the laser at 400 nm. Typically 1 μJ pulses were focused to a ca. 0.1 mm diameter spot at the sample. The probe was produced in a noncollinear optical parametric amplifier and was delayed with respect to the pump using a 1.5 m computer controlled delay line. UV−visible spectra were taken before and after laser exposure to ensure minimal sample degradation and no significant permanent photoproduct formation.

Results and Discussion

Summary of Previous Results and Assignment of the Excited Electronic States. The visible absorption spectra of Cbl(III) species are dominated by several transitions best characterized as $\pi\pi^*$ transitions of the corrin ring, although the Co 3d→ 3d ligand field transitions or Co 3d → corrin π^* MLCT (metal-to-ligand charge transfer) transitions may also contribute.[16−18,40−43] Co 3d → π^* or Co 3d→ 3d transitions also contribute to the long wavelength absorption tail observed for Cbl(II) and Cbl(I) species (see Figure 1).

Excitation of CNCbl and other nonalkylcob(III)alamins results in subpicosecond internal conversion from the initially excited $\pi\pi^*$ state, populating a lower energy excited electronic state, presumably the S_1 state. The population of this S_1 state decays nonradiatively to the ground state on a time scale ranging from a few picoseconds to a few tens of picoseconds. This transition is easily observed in the transient absorption data as the electronic absorption spectrum of the S_1 state is blue-shifted with respect to the ground state spectrum. The lifetime of the excited state was found to correlate with the solvent dielectric constant but not with the solvent viscosity.[21] The excited-state spectrum derived from the transient absorption data is plotted in the left-hand panel of Figure 2. This excited-state spectrum, characterized by a blue shift of the peak of the visible absorption transition along with a red tail, will be designated as a Type I spectrum.

Excitation of MeCbl, EtCbl, and PrCbl results either in direct bond homolysis, presumably from the initially excited $\pi\pi^*$ state, or in rapid internal conversion populating the S_1 excited electronic state. In these alkylcobalamins the S_1 state has a spectrum in the region of the $\alpha\beta$ band similar to that observed for ground state nonalkylcob(III)alamins.[22,24,26,29] The excited-state spectrum derived from the transient absorption data in MeCbl is plotted in the center panel of Figure 2.[22] The S_1 state in EtCbl and PrCbl decays on a 30−50 ps time scale by bond homolysis to form Cbl(II) and an alkyl radical with unit or near unit efficiency. The S_1 state in MeCbl decays on a nanosecond time scale, primarily via internal conversion to the ground state,

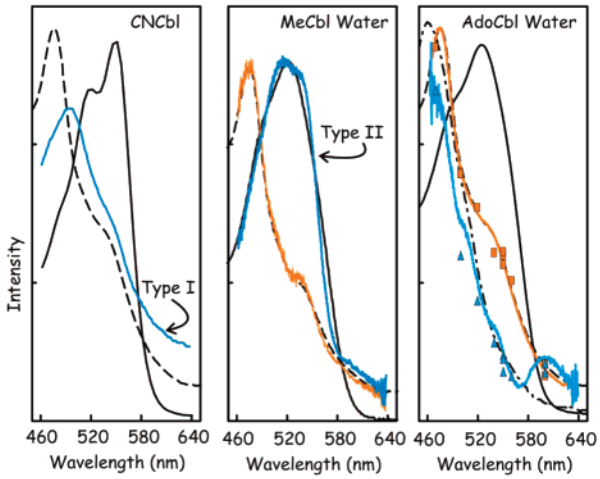

Figure 2. Estimated absorption spectra of intermediate states observed following photolysis of CNCbl, MeCbl, and AdoCbl. The "X"Cbl(III) (solid black lines) and Cbl(II) spectra (dashed black lines) are plotted in each panel. Left: Spectrum of the excited state observed following excitation of CNCbl in water (solid blue line).[21] Center: Spectrum of the long-lived Cbl(III) excited state observed following excitation of MeCbl (blue line) and the Cbl(II) state (orange line) observed following bond dissociation.[22] Right: Spectrum of the intermediate state (ca. 100 ps lifetime, Blue line and triangles) observed prior to bond dissociation and the Cbl(II) state (orange line and rectangles) following excitation of AdoCbl in water. The black dot-dashed line is the spectrum of base-off AdoCbl at pH 2.

but includes a minor pathway (ca. 15%) leading to bond homolysis.[22,24] This excited-state spectrum, characterized by a structured $\alpha\beta$ band peaking between 520 and 540 nm along with an absorption tail extending to the red, will be designated as a Type II spectrum.

Excitation of AdoCbl in water or ethylene glycol leads to rapid internal conversion to an S_1 excited state with a Type I absorption spectrum similar to that observed following excitation of nonalkylcob(III)alamins (*vide infra*). In ethylene glycol solvent this state decays directly to the Cbl(II) bond homolysis product, while in water an additional intermediate precedes bond homolysis.[25] The excited-state spectrum of the additional intermediate state observed for AdoCbl in water is plotted in the right-hand panel of Figure 2.[23,25] The spectral characteristics of this state suggest a weakened bond between the Co and the N ligand supplied by the lower axial dimethylbenzimidazole (DMB) group.

In contrast to AdoCbl in water or ethylene glycol, where the excited-state spectrum is Type I, excitation of AdoCbl bound to GlmES leads to population of an S_1 excited state with a Type II spectrum similar to the excited-state spectrum of MeCbl.[27,28] This state decays by bond dissociation to Cbl(II) on a time scale of *ca.* 100 ps.

The observations outlined above provide insight into the nature of the S_1 state in each case. Earlier studies of Co(II) and Co(III) porphyrins assigned the S_1 state to a ligand-to-metal charge transfer (LMCT) $\pi 3d_{z^2}$ configuration or to a $d_\pi d_{z^2}$ configuration.[44−47] A femtosecond study of tetraphenylporphyrin Co(II)NO demonstrated the ultrafast dissociation of the NO

(40) Day, P. *Coord. Chem. Rev.* **1967**, *2*, 99−108.
(41) Fugate, R. D.; Chin, C.-A.; Song, P.-S. *Biochim. Biophys. Acta* **1976**, *421*, 1−11.
(42) Salem, L.; Eisenstein, O.; Anh, N. T.; Burgi, H. B.; Devaquet, A.; Segal, G.; Veillard, A. *Nouv. J. Chim.* **1977**, *1*, 335−348.
(43) Andruniow, T.; Kozlowski, P. M.; Zgierski, M. Z. *J. Chem. Phys.* **2001**, *115*, 7522−7533.
(44) Tait, C. D.; Holten, D.; Gouterman, M. *Chem. Phys. Lett.* **1983**, *100*, 268−272.
(45) Tait, C. D.; Holten, D.; Gouterman, M. *J. Am. Chem. Soc.* **1984**, *106*, 6653−6659.
(46) Loppnow, G. R.; Melamed, D.; Leheny, A. R.; Hamilton, A. D.; Spiro, T. G. *J. Phys. Chem.* **1993**, *97*, 8969−8975.
(47) Yu, H. Z.; Baskin, J. S.; Steiger, B.; Wan, C. Z.; Anson, F. C.; Zewail, A. H. *Chem. Phys. Lett.* **1998**, *293*, 1−8.

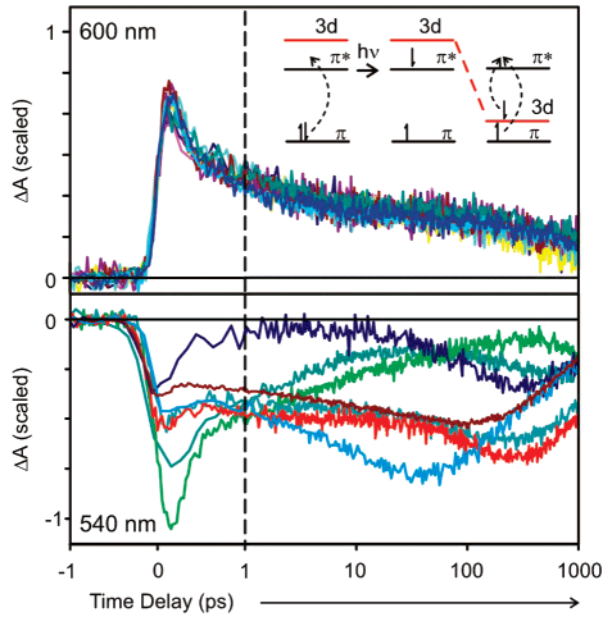

Figure 3. Transient absorption for a variety of alkylcobalamins (MeCbl, EtCbl, PrCbl, AdoCbl) in water, ethylene glycol, and protein (nine samples upper panel, seven samples lower panel). The key for the lower panel is as follows: Dark blue, AdoCbl in GlmES;[28] light blue, AdoCbl in water;[25] brown, AdoCbl in ethylene glycol;[25] red, MeCbl in water;[24] aqua, MeCbl in ethylene glycol;[29] cyan, EtCbl in water;[26] green, PrCbl in water.[26] Data for the same system are plotted in the upper panel, along with EtCbl and PrCbl in ethylene glycol.[29] These plots illustrate the variability in the excited state $\pi\pi^*$ transitions probed at 540 nm contrasted with the uniformity in the ligand field or metal-to-ligand charge transfer transitions probed at 600 nm. The range from −1 to 1 ps is plotted on a linear scale, while 1 ps to 1 ns is plotted on a logarithmic scale. The inset illustrates the stabilization of the Co 3d orbital following excitation resulting in ligand field and $\pi\pi^*$ transitions from the excited state.

ligand with unit quantum yield following excitation at 390 nm.[48,49] This result was attributed to rapid internal conversion from the initially excited $\pi\pi^*$ state of the porphyrin to a directly dissociative $\pi 3d_{z^2}$ LMCT state. The most probable assignment of the lowest excited electronic state in all of the Cbl(III) compounds described above is also to a π3d configuration or possibly to a $(3d/\pi)3d_{z^2}$ configuration where one of the occupied orbitals is a mixture of Co 3d and corrin π.

The ground state spectra are dominated by $\pi\rightarrow\pi^*$ transitions. These strong $\pi\rightarrow\pi^*$ transitions also dominate the excited-state spectra below 580 nm. The differences observed in the 540 nm transient absorption traces plotted in the lower panel of Figure 3 are a consequence of the dependence of these $\pi\rightarrow\pi^*$ transitions on axial ligation and electrostatic environment as illustrated in Figure 1. This assignment, to a configuration involving an electron in a corrin π orbital, rather than a Co $d_\pi d_{z^2}$ LMCT configuration with both electrons on the cobalt, is supported by the similarity of the excited-state spectra to ground state Cbl spectra.

On the other hand, assignment to a configuration involving a Co 3d electron is supported by the insensitivity of the absorption at long wavelengths ($\lambda \geq 600$ nm, top panel of Figure 3) to the evolution between the various intermediate states, including bond cleavage and formation of Cbl(II). Recent DFT calculations identify several long wavelength transitions of Cbl(II).[18,19] These transitions are primarily characterized as Co 3d→3d ligand field transitions or Co 3d → corrin π^* MLCT (metal-to-ligand charge transfer) transitions, although some transitions of corrin π → Co 3d/corrin π^* character are also identified. The assignment of the red absorption to ligand field transitions is consistent with the time-dependent absorption changes. Relaxation of the Cbl(III) following excitation of the initial $\pi\pi^*$ state leads to a stabilization of the 3d orbital on the cobalt as illustrated in the inset of Figure 3. The internal conversion from the initial $\pi\pi^*$ excited state to a $\pi 3d_{z^2}$ state or $\pi 3d_\pi$ state occurs on a subpicosecond time scale (0.2 to 0.6 ps). The 600 nm absorption is insensitive to further change because absorption from the excited state at this wavelength is dominated by Co 3d → π^* or Co 3d→ 3d transitions both in the S_1 excited state and after bond homolysis to produce the Cbl(II) radical.

The assignment of the S_1 state as a π3d LMCT state does not account in a simple manner for the variations observed in the excited-state spectra shown in Figure 2 or for the strong time dependent variations illustrated in the lower panel of Figure 3. The spectral characteristics of the π → π^* transitions are correlated with the interaction between the Co and the axial ligands. In order to clarify the nature of the S_1 excited state for different Cbl(III) compounds, the excited-state lifetime was investigated as a function of temperature and as a function of solvent, using water and ethylene glycol.

Table 1. Excited-state Lifetime of CNCbl as a Function of Temperature

	T (°C)	η^a (mPa s)	ϵ^b	k (ps^{-1})	τ (ps)
water	8	1.39	84.7	0.138	7.25
	21	0.978	79.8	0.152	6.56
	38	0.678	73.9	0.148	6.74
	50	0.547	70.0	0.166	6.02
	63	0.446	65.9	0.176	5.67
ethylene glycol	10	27.5	43.5	0.0617	16.2
	20	19.9	41.3	0.0650	15.4
	40	9.13	37.3	0.0849	11.8
	60	4.95	33.6	0.0994	10.1
	75	3.5	31.1	0.123	8.13

[a] Viscosities from ref 50. [b] Dielectric constants from ref 51.

S_1 Excited State of CNCbl. The lifetime of the excited state of CNCbl was measured as a function of temperature between 8 °C and 75 °C in water and ethylene glycol. At all temperatures the decay is characterized by a subpicosecond component corresponding to internal conversion from the initially excited state to the S_1 state. This internal conversion process depends only very weakly, if at all, on the sample temperature. The picosecond nonradiative decay of the S_1 state to the ground state is temperature dependent, ranging from 7.3 ps at 8 °C to 5.7 ps at 63 °C in water and from 16.2 ps at 10 °C to 8.1 ps at 75 °C in ethylene glycol (Table 1).

These temperature dependent decay rates may be analyzed using an Arrhenius type equation for the rate constant:

$$k = A_h e^{-E_a/RT} \quad (1)$$

Because the excited-state decay is viscosity independent,[21] the dominant contribution to the temperature dependence will be the intrinsic activation energy for decay to the ground state.

(48) Morlino, E. A.; Walker, L. A., II; Sension, R. J.; Rodgers, M. A. J. *J. Am. Chem. Soc.* **1995**, *117*, 4429−4430.
(49) Morlino, E. A.; Rodgers, M. A. J. *J. Am. Chem. Soc.* **1996**, *118*, 11798−11804.
(50) Viscosity of Liquids. In *CRC Handbook of Chemistry & Physics, Internet Version*, 86th ed.; Lide, D. R., Ed.; Taylor and Francis: Boca Raton, FL, 2006.

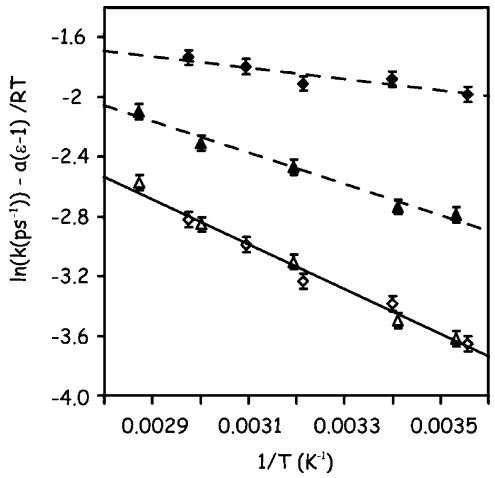

Figure 4. Plot of ln(k) vs 1/T for CNCbl in water (filled diamonds, dashed line) and ethylene glycol (filled triangles, dashed line), ln(k) − $a(\epsilon - 1)$/RT in water (open diamonds) and ethylene glycol (open triangles). The value for a is 0.0466 kJ/mol per unit change in dielectric constant as described in the text.

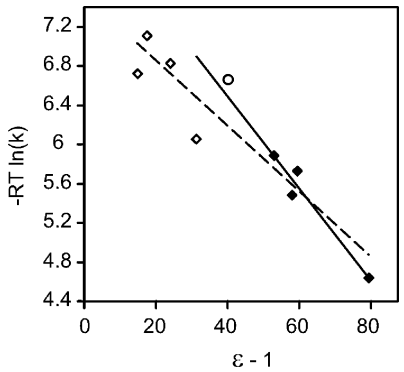

Figure 5. $-RT$ ln(k) (in kJ/mol) vs dielectric constant ($\epsilon - 1$) for CNCbl at room temperature in a variety of solvents and solvent mixtures. There is a clear correlation with solvent polarity although the scatter is also significant. The filled diamonds represent data obtained in water or 50/50 mixtures of water and ethanol, methanol, or acetonitrile.[21] The open diamonds represent data obtained in neat alcohol solvents, methanol, ethanol, 2-propanol, and isobutanol.[21] The circle is the data point obtained in ethylene glycol in the present study. The dashed line is a linear fit to all of the data; the solid line is a linear fit to the filled diamonds.

Assuming that both A_h and the activation energy are temperature independent, an activation energy barrier may be extracted from the slope of a plot of ln(k) vs 1/T.

$$\ln(k) = -\frac{E_a}{RT} + \ln(A_h) \qquad (2)$$

Linear fits to the data are plotted in Figure 4. The slope of the temperature dependence in ethylene glycol is approximately three times as steep as the slope in water corresponding to a much larger barrier for internal conversion. The apparent barrier is 8.7 ± 0.7 kJ/mol (727 ± 55 cm^{-1}) in ethylene glycol but only 3.2 ± 0.8 kJ/mol (265 ± 65 cm^{-1}) in water.

However, the assumption that E_a is temperature independent is questionable. The lifetime of the CNCbl excited state was shown in an earlier study to correlate with the solvent dielectric constant.[21] Thus the interpretation of a plot of ln(k) vs 1/T is complicated by the temperature dependence of the solvent dielectric constant. Over the temperature range investigated here the dielectric constant of water ranges from 84.7 at 281 K to 65.9 at 336 K, a 22% decrease. The dielectric constant in ethylene glycol ranges from 43 at 283 K to 31 at 348 K, a 27% decrease.[51] Temperature dependent changes in solvent polarity will modify the electronic state energy[52,53] and thus the activation energy for internal conversion.

If the entire dependence of rate on dielectric constant is in the influence of solvent polarity on the activation barrier, a plot of RT ln(k) vs $\epsilon - 1$ at constant temperature will highlight the dependence of activation energy on the dielectric constant. The function $-RT$ ln(k) vs $\epsilon - 1$ at constant temperature is plotted in Figure 5 for CNCbl in a range of solvents. A linear fit accounts for the trends observed in the data predicting a decrease in activation energy of 0.033 ± 0.005 kJ/mol per unit increase in the dielectric constant. A linear fit to the high dielectric constant data predicts a decrease in activation energy of 0.047 ± 0.005 kJ/mol per unit increase in the dielectric constant.

This linear dependence of E_a on the dielectric constant may be incorporated into an analysis of the temperature dependence in both water and ethylene glycol.

$$\ln(k) - \frac{a(\epsilon - 1)}{RT} = -\frac{E_a^1}{RT} + \ln(A_h) \qquad (3)$$

where $E_a(\epsilon) = E_a^1 - a(\epsilon - 1)$ and E_a^1 is the barrier extrapolated to vacuum ($\epsilon = 1$). If the only factor influencing the barrier is the electrostatic stabilization of the energy of the excited state, plots of the data in water and ethylene glycol should collapse to the same slope and intercept. This is the case, as illustrated in Figure 4. The value for a which minimizes the deviation from a straight line is 0.0466 kJ/mol per unit change in dielectric constant. This value is in excellent agreement with the slope obtained from the high dielectric constant data in Figure 5. Analysis of the data using eq 3 yields an extrapolated gas phase activation energy of 12.5 ± 0.5 kJ/mol. The barriers obtained from the slopes of a plot of ln(k) vs 1/T are much smaller, reflecting the fact that the barrier increases as the temperature increases.

The picture emerging from the data is an excited electronic state that involves a modest charge redistribution. The energy of this state is stabilized by solvent reorganization as sketched in Figure 6a. The behavior of the excited electronic state is consistent with a π3d LMCT state with charge transfer from the π orbitals of the corrin ring to the central Co atom and a concomitant weakening of the Co−C bond. The internal conversion involves a charge rearrangement and is essentially independent of the dynamical properties of the solvent.

S_1 Excited State of MeCbl. In contrast to CNCbl described above, a distinctively different excited electronic state spectrum is observed subsequent to excitation of the following: MeCbl in water, in ethylene glycol, or bound to methionine synthase;[22,24,29] EtCbl and PrCbl excited at 520 nm in water;[26] and AdoCbl when bound to glutamate mutase (GlmES).[27,28] The excited state is long-lived for MeCbl, with lifetimes of 1 and 2.4 ns at room temperature in water and ethylene glycol,

(51) Permittivity (Dielectric Constant) Of Liquids. In *CRC Handbook of Chemistry & Physics*, *Internet Version*, 86th ed.; Lide, D. R., Ed.; Taylor and Francis: Boca Raton, FL, 2006.
(52) Zhao, X.; Burt, J. A.; Knorr, F. J.; McHale, J. L. *J. Phys. Chem. A* **2001**, *105*, 11110−11117.
(53) Zhao, X.; Knorr, F. J.; McHale, J. L. *Chem. Phys. Lett.* **2002**, *356*, 214−220.

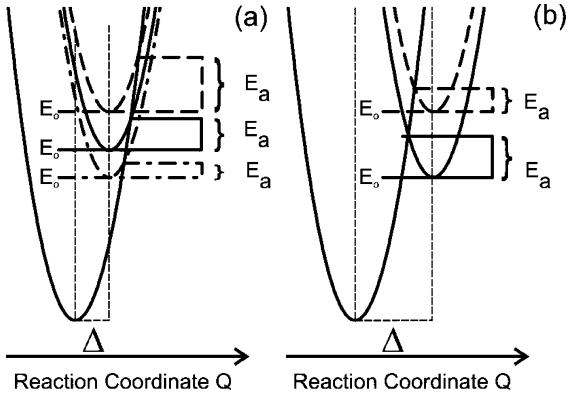

Figure 6. This cartoon illustrates the influence of solvent stabilization on the activation energy for internal conversion. (a) For a modest charge redistribution a polar solvent will stabilize the energy of the excited state leading to a lower activation energy for internal conversion. (b) For larger displacements a polar solvent will stabilize the energy of the excited state leading to a higher activation energy for internal conversion.

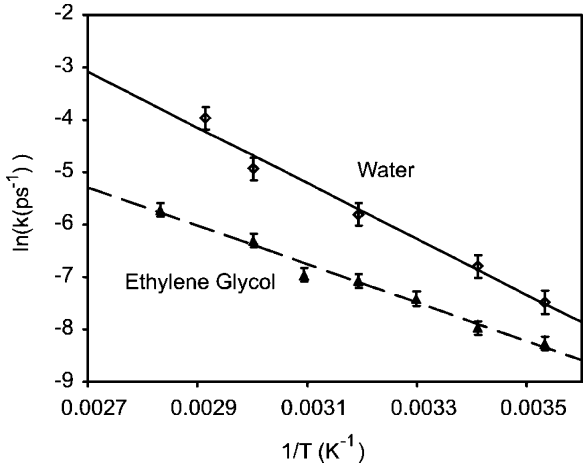

Figure 7. Plot of ln(k) vs $1/T$ for MeCbl in water (diamonds, solid line) and ethylene glycol (triangles, dashed line).

respectively, but much shorter-lived for EtCbl (48 ps) and PrCbl (32 ps) in water and for AdoCbl bound to GlmES (105 ps). While the lifetime is strongly dependent on the specific alkyl group, it should be noted that the spectral features are not dependent on the alkyl group. This intermediate state is characterized by an absorption spectrum with a pronounced $\alpha\beta$ band structure, resulting in a difference spectrum with an easily identified characteristic shape.[22,24,26−28]

The Type II excited-state spectrum is similar to the ground state spectrum of six-coordinate Cbl(III) compounds, with a $\alpha\beta$ structure more like that observed for nonalkylcob(III)alamins than for alkylcob(III)alamins. Thus the spectrum is characteristic of a Cbl(III) species with a σ-donating alkyl anion ligand, rather than a Co−C covalent bond.[22] The intermediate state observed in these alkylcobalamins is better characterized as a metal-to-ligand charge transfer (MLCT) state, corrin $\pi \rightarrow$ Co $\rightarrow$ R, in contrast to the LMCT excited state (corrin $\pi \rightarrow$ Co) observed following excitation of the typical nonalkylcob(III)alamins or following the excitation of AdoCbl in water, although it is likely that the state remains nominally a π3d state.

To further probe the nature of the Type II excited state, the temperature dependence of the lifetime for MeCbl in water and ethylene glycol was measured between 10 °C and 70 °C (water) or 80 °C (ethylene glycol). The apparent barrier in water (44 ± 3 kJ/mol) is higher than the barrier in ethylene glycol (30 ± 2 kJ/mol), although the rate of internal conversion is faster in water than EG (Figure 7). The increase in activation energy with an increase in solvent polarity is consistent with an excited electronic state that has significant charge-transfer character. Electron transfer from the cobalt to the axial ligand, as suggested by the structure in the absorption band, induces a change in the solvent and/or within the Cbl molecule. In this case the system resembles the plot in the right-hand panel of Figure 6. Solvent polarity stabilizes the excited state and thus increases the barrier for ground state recovery.

Unlike CNCbl, the correlation between the static dielectric constant of the solvent and the energy of the excited state cannot account for the entire dependence of the rate constant on solvent. Analysis of the data according to eq 3 leads to a value for a which is capable of collapsing the data to parallel lines having the same slope but different intercepts. The value for a which minimizes the deviation in the slopes of the lines is −0.168 kJ/mol per unit change in the dielectric constant and E_a^1= 14.4 ± 3.6 kJ/mol. The intercepts obtained from the fits are ln(A_h) = 0.78 ± 0.71 (ethylene glycol) and 4.5 ± 1.4 (water) leading to A_h = 2.2 ps^{-1} (error range 1.1 to 4.5 ps^{-1}) in ethylene glycol and 90 ps^{-1} (error range 22 to 370 ps^{-1}) in water. If the principal influence of solvent on A_h is the dynamical solvent reorientation the pre-exponential factor should be proportional to $1/\tau_s$ where τ_s is the time scale for solvent reorientation.[54] Experimental measurements of solvent reorientation yield values of $\langle\tau\rangle_{obsd}$ = 0.34 ps in water and 15 ps in ethylene glycol.[55] The ratio of these values ($0.34^{-1}/15^{-1} = 15/0.34 = 44$) is in good agreement with the ratio of the extrapolated values for A_h = (90/2.2 = 41).

This analysis ignores the influence of temperature on the solvent dynamics but nonetheless provides a good qualitative understanding of the ground state recovery. All of the available data points to an S_1 excited state with substantial charge transfer to the CH_3 group. The $\alpha\beta$ band is similar to that observed for ground state anion ligands, as is the UV γ band absorption.[22] The temperature dependence and polarity dependence of the ground state recovery are consistent with a back electron transfer process.

S_1 Excited State of AdoCbl. Excitation of AdoCbl in water or in ethylene glycol is followed by a progression through two or three short-lived intermediate states, followed by bond homolysis with unit or near unit quantum yield. The species associated spectra for the intermediates observed in water and ethylene glycol are summarized in Figure 8. The temperature dependence of the rate constants in both ethylene glycol and water solvents are plotted in Figure 9. The fastest time constant plotted here, rate constant k_1, is essentially independent of solvent and represents a blue shift of the excited-state spectrum. This conversion from state 1 to state 2 may involve a conversion between two excited states as sketched in the upper panel of Figure 9 or may represent relaxation of the molecule in the populated electronic excited state. In either case, the spectra of the early intermediates in both water and ethylene glycol (red and green lines) are Type I, suggestive of the population of an excited state with weakened axial ligands. The observed spectra

(54) Cukier, R. I.; Nocera, D. G. *J. Chem. Phys.* **1992**, *97*, 7371−7376.
(55) Maroncelli, M. *J. Chem. Phys.* **1997**, *106*, 1545−1555.

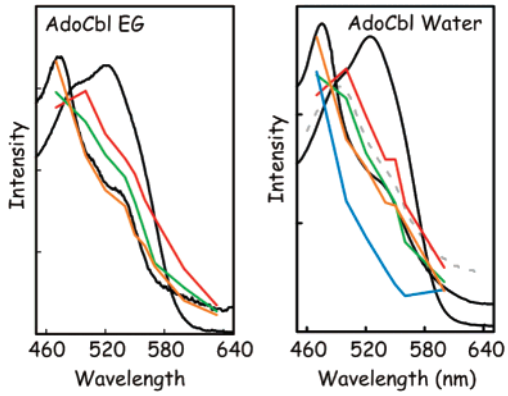

Figure 8. Species associated spectra deduced from global analysis of transient spectral changes observed for AdoCbl.[25] Left: AdoCbl in ethylene glycol. Red (1−2 ps lifetime at room temperature) and green lines (25−35 ps lifetime at room temperature) represent the spectra of the two early intermediates observed prior to the development of a spectrum characteristic of Cbl(II) shown in orange. Right: AdoCbl in water. The first two intermediates in water resemble those observed in ethylene glycol and have similar lifetimes (ca. 1−2 ps red, 20 ps green at room temperature); however a third intermediate with a blue-shifted absorption spectrum is also observed in water (ca. 130 ps lifetime at room temperature). For comparison the ground state AdoCbl and Cbl(II) spectra (solid black lines) and the excited-state spectrum of CNCbl in water (gray dashed line) are also shown.

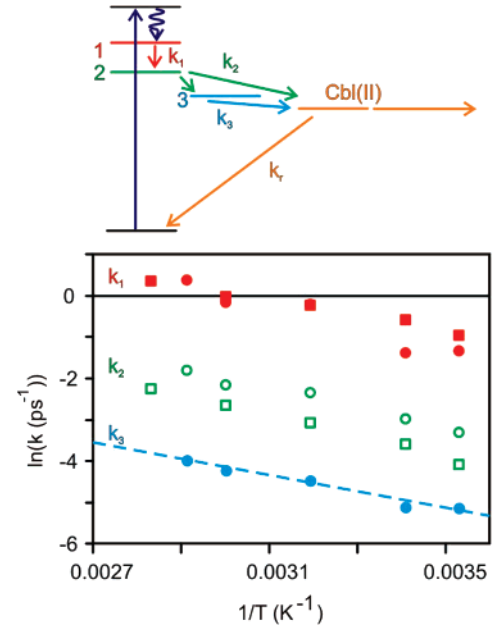

Figure 9. ln(k) vs 1/T for AdoCbl in water (circles) and ethylene glycol (squares). The rate constants are color coded to the model and to the species associated spectra plotted in Figure 8.

are similar to those observed for the CNCbl (Figure 2) and the other nonalkyl Cbl(III) species,[21] reflecting population of a π3d LMCT state.

In ethylene glycol at room temperature the formation of a Cbl(II) spectrum from the intermediate state 2 occurs on a 28 ps time scale. In earlier work at room temperature an additional ca. 100 ps component was identified. However this time constant correlated with small changes in a Cbl(II)-like spectrum and is not easily identified at all temperatures. The data are adequately modeled without this component. The apparent barrier for bond dissociation is 21.0 ± 1.1 kJ/mol, although given the influence of solvent polarity on the energy of the π3d LMCT state in CNCbl, it is clear that this barrier may be modified somewhat by the temperature dependent change in the polarity of ethylene glycol.

Excitation of AdoCbl in water leads to similar spectral evolution at early times as described above but is followed by formation of an additional intermediate state not observed in ethylene glycol. The spectrum of this state (blue line in the right-hand panel of Figure 2 and in the right-hand panel of Figure 7) is consistent with further weakening or dissociation of an axial nitrogenous ligand. The spectrum is blue-shifted with respect to the Cbl(II) spectrum and approaches that observed following dissociation of the dimethylbenzimidazole (DMB) base (base-off spectrum)[25] with the addition of a red absorption band assigned to Co 3d → π*/3d transitions as shown in Figure 2. The excited-state spectrum likely reflects stabilization of the π3d LMCT state through solvation of the lower axial DMB base. Bond dissociation from this state occurs on a time scale of 100 ps at room temperature, ranging from ca. 150 to 50 ps as the temperature increases from 10 °C to 70 °C. The Arrhenius plot in Figure 9 suggests an apparent activation energy of ca. 16.3 ± 1.6 kJ/mol for the decay of this intermediate to the bond homolysis Cbl(II) photoproduct. Again, this barrier may be modified somewhat by the temperature dependent change in the polarity of the solvent.

Summary and Conclusions

The S_1 excited electronic state populated following excitation of both alkyl and nonalkyl Cbl(III) compounds is a state best characterized as a $\pi 3d_{z^2}$ or $\pi 3d_{\pi}$ state. The excited-state absorption exhibits transitions characteristic of ground state $\pi \rightarrow \pi^*$ excitations, with the addition of a red absorption tail characteristic of ligand field transitions from the Co 3d orbitals. This state is well characterized as a corrin $\pi \rightarrow$ Co or corrin $\pi \rightarrow$ Co → R CT state.

The $\pi \rightarrow \pi^*$ transition of the S_1 excited state of CNCbl is blue-shifted from the ground state $\pi \rightarrow \pi^*$ transition of Cbl(III) compounds in a manner characteristic of a weakened interaction with the axial ligand. The excited state is stabilized by increasing solvent polarity, but the stabilization is relatively small and there is no indication that solvent reorientation plays any role in the internal conversion from the S_1 state to the ground state. The S_1 state of AdoCbl in both water and EG is also blue-shifted from the ground state $\pi \rightarrow \pi^*$ transition of Cbl(III) compounds in a manner characteristic of a weakened interaction with the axial ligand. Solvation of the chromophore in water, likely solvation of the DMB base, leads to a blue shift and further stabilization of the S_1 state.

In contrast, the spectra of the S_1 states of MeCbl, EtCbl, and PrCbl resemble the ground state spectra observed for nonalkylcob(III)alamins, with a pronounced $\alpha\beta$ structure. The S_1 state is characterized by a significant charge redistribution. The molecular orbitals calculated for MeCbl exhibit a substantial mixing of the Me $2p_z$ and Co $3d_{z^2}$ orbitals, while the orbitals calculated for H_2OCbl and CNCbl are more heavily localized on the Co.[17] The change in charge distribution within the nominal Co $3d_{z^2}$ influences the spectrum of the excited state, the energy of the excited state as a function of electrostatic environment, and the dynamics of the internal conversion or bond dissociation processes depopulating the excited state.

It is important to note that the S_1 state spectrum of the various cob(III)alamins investigated in this work either resembles that

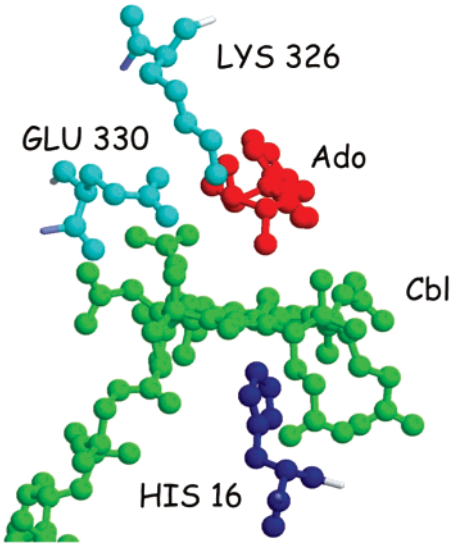

Figure 10. Structure of AdoCbl bound to glutamate mutase.[56] Two amino acids, Glu 330 and Lys 326, are within hydrogen-bonding distance of the adenosyl group.

observed in CNCbl with a pronounced blue shift characteristic of weakened axial ligation (Type I) or exhibits the pronounced $\alpha\beta$ band characterized by an absorption peak around 540−550 nm (Type II). In no case is a gradual change from one spectral type to the other observed. On the other hand, the lifetimes may vary dramatically, from 1 ps or less to 100 ps for the Type I spectrum and from 30 ps to 2.5 ns for the Type II spectrum. The differences in the electronic spectra of the S_1 $\pi 3d_{z^2}$ state as a function of the axial ligand manifests changes in the mixing of the ligand 2s and $2p_z$ and Co $3d_{z^2}$ orbitals, while changes in the absolute rates for reaction reflect stabilization or destabilization of the S_1 state as a function of electrostatic environment or as a function of the σ-donating strength of the axial ligand.

When AdoCbl is bound to glutamate mutase the S_1 spectrum is modified to resemble the spectrum observed for MeCbl, EtCbl, and PrCbl. The electrostatic influence of the GlmES environment does not simply modify the energy of the S_1 $\pi 3d$ state. Rather the influence of electrostatic environment is to modify the nature of the excited state from Type I to Type II. The above analysis suggests that the electrostatic environment of the protein influences the mixing of the C 2s and 2p orbitals with the Co $3d_{z^2}$ orbital and increases the charge-transfer character of the excited-state stabilizing partial negative charge on the adenosyl group.

The results reported here suggest the need for a careful theoretical comparison of the electronic structure and spectra of Cbl(III) compounds as a function of alkyl ligand. Clearly calculations of MeCbl analogues should not be considered adequate models for AdoCbl. The influence of the protein environment on the electronic structure of AdoCbl also suggests that specific interactions between the Ado group and the protein may play an important role in controlling the reactivity. X-ray crystal structures of glutamate mutase reveal two amino acids, Glu 330 and Lys 326, within range for direct hydrogen bonding interactions with the hydroxyl groups on the ribose ring of the adenosyl group (Figure 10).[56] The influence of the protein may result from the general electrostatic environment or from the modification in the electronegativity of the Ado group arising from these specific interactions.

Acknowledgment. This research was funded in part by the NSF through Grant CHE-0078972.

JA066197Y

(56) Gruber, K.; Reitzer, R.; Kratky, C. *Ang. Chemie IE* **2001**, *40*, 3377−3380.